Published in final edited form as:
J Comp Neurol. 2005 May 16; 485(4): 280–292. doi:10.1002/cne.20481.

Exuberant Thalamocortical Axon Arborization in Cortex-Specific NMDAR1 Knockout Mice

LI-JEN LEE[1], **TAKUJI IWASATO**[2,3], **SHIGEYOSHI ITOHARA**[3], and **REHA S. ERZURUMLU**[1,*]

[1]Department of Cell Biology and Anatomy, Louisiana State University Health Sciences Center, New Orleans, Louisiana 70112

[2]Precursory Research for Embryonic Science and Technology, Japan Science and Technology Agency, Saitama 332-0012, Japan

[3]Laboratory for Behavioral Genetics, RIKEN Brain Science Institute, Saitama 351-0198, Japan

Abstract

Development of whisker-specific neural patterns in the rodent somatosensory system requires NMDA receptor (NMDAR)-mediated activity. In cortex-specific *NR1* knockout (Cx*NR1*KO) mice, while thalamocortical afferents (TCAs) develop rudimentary whisker-specific patterns in the primary somatosensory (barrel) cortex, layer IV cells do not develop barrels or orient their dendrites towards TCAs. To determine the role of postsynaptic NMDARs in presynaptic afferent development and patterning in the barrel cortex, we examined the single TCA arbors in Cx*NR1*KO mice between postnatal days (P) 1–7. Sparsely branched TCAs invade the cortical plate on P1 in Cx*NR1*KO mice as in control mice. In control animals, TCAs progressively elaborate patchy terminals, mostly restricted to layer IV. In Cx*NR1*KO mice, TCAs develop far more extensive arbors between P3–7. Their lateral extent is twice that of controls from P3 onwards. By P7, Cx*NR1*KO TCAs have significantly fewer branch points and terminal endings in layers IV and VI but more in layers II/III and V than control mouse TCAs. Within expansive terminal arbors, Cx*NR1*KO TCAs develop focal terminal densities in layer IV, corresponding to the rudimentary whisker-specific patches. Given that thalamic NMDARs are spared in Cx*NR1*KO mice, the present results show that postsynaptic NMDARs play an important role in refinement of presynaptic afferent arbors and whisker-specific patterning in the developing barrel cortex.

Indexing terms

barrels; barreloids; trigeminal system; somatosensory cortex; region-specific gene knockout

A conspicuous feature of the rodent primary somatosensory cortex is the presence of neural patterns within face and digit representation regions of the body map. Patches of thalamocortical afferent (TCA) arbors and their postsynaptic partners form discrete modules that replicate the patterned distribution of whiskers on the contralateral snout. These cellular modules are termed “barrels” (Woolsey and Van der Loos, 1970). Whisker and digit-related patterns are first established in the brainstem somatosensory nuclei, then in the ventrobasal nuclear complex (VB) of the dorsal thalamus, and finally in the layer IV of the neocortex. Such cellular modules are called “barreloids” in the VB, and “barrelettes” in the brainstem (Woolsey and Van der Loos, 1970; Van der Loos, 1976; Ma and Woolsey, 1984). The

*Correspondence to: Reha S. Erzurumlu, Dept. Cell Biology and Anatomy, LSUHSC, 1901 Perdido St., New Orleans, LA, 70112. rerzur@lsuhsc.edu.

instructive role of the sensory periphery in sculpting central neural patterns has been demonstrated by lesion studies performed in perinatal rodents, or in mice selectively bred for aberrant numbers of whiskers (Welker and Van der Loos, 1986; Woolsey, 1990; O'Leary et al., 1994; Killackey et al., 1995). Several lines of evidence also indicate that somatosensory periphery-related neural maps and patterns are conveyed to target cells by the afferents at each synaptic relay station (Erzurumlu and Jhaveri, 1990, 1992a, b; Senft and Woolsey, 1991).

In recent years, a number of transgenic and knockout (KO) mouse models have begun yielding clues to the underlying mechanisms of pattern formation in the rodent somatosensory system, with profound implications for other sensory pathways in the mammalian brain. Current understanding is that topographically organized projections (somatotopic maps) along the somatosensory system are established via a number of axon guidance cues (Erzurumlu et al., 1990; Maier et al., 1999; Grove and Fukuchi-Shimogori, 2003; López-Bendito and Molnár, 2003; Vanderhaeghen and Polleux, 2004). On the other hand, patterning of neural connections within "somatotopic" maps is controlled by neural activity-mediated mechanisms (Erzurumlu and Kind, 2001). In this phase of somatosensory system development, glutamatergic transmission occupies the center stage. The results of numerous pharmacological blockade and genetic manipulation studies support the conclusion that N-methyl-D-aspartate receptor (NMDAR)-mediated neural activity plays a major role in refinement of neural connections and plasticity of vertebrate sensory pathways. In the mouse somatosensory system, whisker-specific neural patterns are absent following mutations of the NMDAR subunits NR1 (Li et al., 1994; Iwasato et al., 1997) or NR2B (Kutsuwada et al., 1996). Cortex-specific *NR1*KO (Cx*NR1*KO) mice were generated using the Cre/loxP system; the *NR1* gene is deleted by expression of Cre recombinase in the *Emx1*-positive excitatory cortical neurons but not in the GABAergic inhibitory neurons (Iwasato et al., 2000). In these animals, while subcortical neural patterns representing the whiskers are normal, layer IV stellate cells do not orient their dendrites or form barrels (Iwasato et al., 2000; Datwani et al., 2002a). Only those TCAs representing the large whiskers form rudimentary patterns and display critical period plasticity similar to that seen in wildtype (WT) mice (Iwasato et al., 2000; Datwani et al., 2002b).

We performed detailed analyses of TCA development in the barrel cortex of Cx*NR1*KO mice. Single axon analyses between postnatal days (P) 1–7 revealed that while whisker-specific TCAs target proper cortical layers at first and begin arborization similar to that seen in controls, their growth is not confined to layer IV. These axons develop exuberant arbors in multiple cortical layers and fail to consolidate their terminal arbors into patches within layer IV. In addition to branching and forming terminals in multiple layers, TCAs develop wider arbors along the mediolateral extent of the mutant barrel cortex. Despite these large arbors, zones of terminal condensations are seen in layer IV. These terminal condensations correspond to the rudimentary patterning seen with histochemical and immunohistochemical markers.

MATERIALS AND METHODS

Generation and genotyping of Cx*NR1*KO mice

Cx*NR1*KO mice were generated as described previously (Iwasato et al., 2000). These mice were obtained by crossing $Emx1^{Cre/+}NR1^{+/-}$ or $Emx1^{Cre/Cre}NR1^{+/-}$ mice with $NR1^{flox/flox}$ mice. Out of four types of offspring, $Emx1^{Cre/+}NR1^{flox/-}$ mice were Cx*NR1*KO, others ($Emx1^{+/+}NR1^{flox/-}$, $Emx1^{Cre/+}NR1^{flox/+}$, or $Emx1^{+/+}NR1^{flox/+}$) were used as controls. Mice were genotyped by tail sample PCR as described before (Iwasato et al., 2000). All animal handling was in accordance with the protocols approved by the Animal Use and Care Committees of the Louisiana State University Health Sciences Center and RIKEN BSI.

Histology and axonal labeling

Postnatal (P1, P3, P5, and P7) mice were given an overdose of sodium pentobarbital and perfused transcardially with 4% paraformaldehyde in 0.1 M phosphate buffer (PB), pH 7.4. Brains were removed and cut transversely between the inferior and superior colliculi and kept in the same fixative for 1–2 days. Cortices of some brains were removed and flattened between two glass slides.

For serotonin (5-HT) transporter (5-HTT) immunohistochemistry, 50 μm (P1), 60 μm (P3), or 100 μm (>P5) thick tangential sections were taken from flattened cortices. After 1 hour 4% normal goat serum blocking, the sections were incubated overnight in anti 5-HTT rabbit polyclonal antibody (1:10,000, Diasorin, Stillwater, MN) in PB with 3% Triton X-100. Sections were then rinsed in PB, incubated in a secondary antibody solution (biotinylated goat antirabbit, 1:200; Sigma, St. Louis, MO), and processed using an ABC kit (Vector Laboratories, Burlingame, CA) and 3,3′-diaminobenzidine (DAB, Sigma). In this part of the study, a minimum of five animals were used for each age and genotype.

Previous studies have used a nonconventional plane of forebrain sectioning in order to obtain slices that contain VB, its projections, and the barrel cortex (Agmon and Connors, 1991; Senft and Woolsey, 1991; Agmon et al., 1995; Rebsam et al., 2002). Here, we further optimized cutting angles for each age to obtain single brain sections that contain largely intact thalamocortical pathway in the developing brain (Fig. 1, Table 1). For this purpose, a total of 128 WT, control, and Cx*NR1*KO mice ages P1, P3, P5, and P7 were used. First, the forebrains were split in half along the sagittal plane and embedded in 2% agar with the medial side down. Second, the specimen was placed on a transparency with an X-Y coordinate. The posterior pole of the cortex was placed on the transparency contacting the Y-axis and the plane along the olfactory bulb and the base of the forebrain was aligned with the X-axis as illustrated in Figure 1B. Different angles (15, 20, 25, or 30° away from the X-axis) of trimming the agar block were tested (Fig. 1). The specimen blocked in agar was lifted and cut in oblique angles (45, 50, 55, or 60° away from the Y-axis were tested). Finally, the block was mounted with the rostral pole of the brain down onto the stage of the vibratome (VT1000S, Leica, Nussloch, Germany) and sectioned.

Alternate sections of 400 and 100 μm thickness were cut and reacted for cytochrome oxidase (CO) histochemistry (0.5 mg/ml Type III cytochrome C, Sigma, 0.5 mg/ml DAB, and 40 mg/ml sucrose in PB, pH 7.4). After the barreloids in the VB were visualized, the 400-μm section was rinsed in PB and a tiny (15–20 μm in diameter) crystal of DiI (1,1′-dioctodecyl-3,3,3′,3′-tetramethylindocarbocyanine perchlorate, Molecular Probes, Eugene, OR) was picked with a glass pipette with a tip of 20 μm and inserted into a single barreloid in the large whisker representation area (Fig. 1). The section was then transferred to PB containing 4% paraformaldehyde and kept at 37°C in the dark for 5–8 days for dye diffusion. The adjacent CO-stained 100-μm section was used for the comparison of cortical layers and barrel patterns. DiI-labeled sections were viewed under an epifluorescence microscope using a rhodamine filter set. Numerous fibers with their terminals were then imaged at different focal planes and the images acquired using a CoolSnap digital camera (US Photometrics, Tucson, AZ). Each image was magnified and single axons and their arbors were reconstructed by tracing them from the computer screen. Multiple images and drawings of axonal processes from serial images were then reconstructed.

For single TCA DiI labeling study, we used 226 brains (see Table 1) from P1, P3, P5, and P7 Cx*NR1*KO and control mice. Two to three slices were collected from each hemisphere for DiI labeling. Usually one or two slices from each hemisphere had intact and isolated TCAs. Despite the large numbers of animals used, numbers of recovered single TCAs were relatively low but high enough for statistical analyses and comparisons. Numbers of traced

TCAs included in morphometric analyses are shown in Table 1. These axons were traced and reconstructed without prior knowledge of the genotype of the animal from which the brain slice was derived.

For verification of layers in CO-stained sections, a series of brains of control (n = 8) and experimental (n = 8) animals at P1, P3, P5, and P7 were cryoprotected in sucrose and sectioned at an optimal angle on a freezing microtome at 60 μm thickness. Serial sections were collected in 24-well plates and alternate sections were reacted for CO histochemistry and stained with cresyl violet. Both series of sections were dehydrated through a series of graded alcohols and xylenes and coverslipped with per-mount.

Quantification and data analyses

Due to inherent difficulties in sorting out branches and arbors of overlapping axons when two or more labeled parent axons are present in a given section, we only used cases where a single axon could be traced from the internal capsule. Optimization of section angles for each age allowed us to reconstruct the terminal branches of each single axon within a 400-μm-thick section. While most of the tips of the traced terminal branches had bouton-like endings, we cannot rule out the possibility that some of the terminal branches were cut. However, we feel that by analyzing large numbers of axons, accurate comparisons between the Cx*NR1*KO and control TCAs can be made, even though the absolute numbers of branches and terminal tips remain undetermined. Axonal processes were measured from the reconstructed 2D display of single TCAs in both control and Cx*NR1*KO animals ages P1, P3, P5, and P7. The mediolateral extent of each individual afferent arbor was measured. Bifurcation points and terminal tips of each reconstructed single TCA were counted in each cortical layer determined by CO histochemistry. Additional quantitative analyses and comparisons were done by calculating the total number of branch points, terminal tips, and total axonal length after the first branch point of the terminal field of all reconstructed single axons for each age between experimental and control groups. Arbor density was determined by counting intersections across the two diagonals of every 25 × 25-μm square. Student's *t*-test was used for testing the variation of mean values.

Photomicrographs

All samples were analyzed with a Nikon DIAPHOT 300 microscope. Photomicrographs were captured with a Cool-Snap digital camera using MetaVue image software (Universal Imaging, Downingtown, PA). The images were adjusted for brightness and contrast using Adobe PhotoShop 7.0 (San Jose, CA) software on a PC computer. For Figure 4, images from consecutive optical sections of the same preparation were merged to form montages. No other alterations were made.

RESULTS

The emergence of whisker-specific patterning in the control and Cx*NR1*KO mice barrel cortex was visualized with 5-HTT immunohistochemistry as early as P3 (Fig. 2). Because developing TCAs transiently express 5-HTT, it has been used as a reliable marker for developing TCAs for the somatosensory, visual, and auditory systems (Lebrand et al., 1996, 1998; Rebsam et al., 2002). This marker for TCAs and a common barrel pattern marker, CO histochemistry, show the emergence and consolidation of whisker-specific TCA patterns in the mouse barrel cortex between P3–7 (Figs. 2, 3). In Cx*NR1*KO mice, these patterns emerge during the same period as in control mice, but are present for only the large whisker TCAs. In addition, these individual patches are much smaller and interpatch distances are wider than controls.

At the morphological and physiological levels, the thalamocortical pathway of mice is best analyzed using brain slices that contain VB and its projections to the cortical target fields (Agmon and Connors, 1991; Senft and Woolsey, 1991). These slices are cut at an oblique angle parallel to the trajectory of the thalamocortical axons. However, since the forebrain structures change in size and shape during the postnatal period, we first modified the parameters of oblique sectioning of the brain to obtain an intact thalamocortical pathway slice for P1, 3, 5, and 7 mouse brains. These ages in mice correspond to invasion of the cortical plate by TCAs, their initial phases of patterning, consolidation of barrel patterns, and after the end of the critical period for structural plasticity, respectively. In order to obtain an optimal angle for thalamocortical slices, several different angle combinations were tested for each age group (Fig. 1). For P1, 20–50, 20–55, 20–60, 25–50, 25–55, and 30–55; for P3, 20–50, 20–55, and 25–50; for P5, 25–55, 30–55, and 30–60; for P7, 25–55 and 25–60 (in degrees, deviated from X-axis and Y-axis, respectively) are good angle combinations and are summarized in Figure 1E. The optimal angles were similar for both control and KO brains.

In order to determine whether small patches of TCAs seen with 5-HTT immunohistochemistry and CO histochemistry correspond to small terminal arbors of TCAs in Cx*NR1*KO mice, we examined single TCAs by labeling them from optimized thalamocortical slices. A separate series of alternate sections from thalamocortical slices of control and Cx*NR1*KO mice were prepared and stained for CO and Nissl. Comparison of cytoarchitecture of the developing control and Cx*NR1*KO cortex with CO staining (Fig. 3) allowed us to delineate specific cortical layers in DiI-labeled material. We visualized whisker barreloids in the thalamus by CO staining of thalamocortical slices, and inserted a tiny DiI crystal in a single barreloid at P3, 5, and 7 (Fig. 1F). At P1, barreloids are not visible with CO staining yet, but the outline of the VB is already clear. Therefore, at this age we placed small DiI crystals into the presumptive barreloid region of the VB visualized by CO staining. Typical examples of DiI-labeled single TCAs against a backdrop of CO-stained patches are illustrated in Figure 4. Since these thalamocortical slices are in an oblique coronal plane, our analyses and reconstructions of single axons were restricted to the mediolateral axis of TCA terminal fields. We were not able to assess the extent of the TCA terminal fields along the rostrocaudal axis of the barrel field. Typical examples of single axons reconstructed from control and Cx*NR1*KO groups, for each age, are shown in Figure 5.

At P1, TCAs invade the cortical plate as simple axons with few small branches. Their morphological appearance is similar in both control and Cx*NR1*KO mice (Fig. 5A). On P3, TCAs of the control animals display focalized branches in layer IV and to a lesser extent in layer VI. Very few branches are seen in other layers. In Cx*NR1*KO cortex, TCAs display a wider terminal territory and more branches in other layers (Fig. 5B). At P5 and on, as the normal TCAs consolidate their focal terminal arbors in layer IV and fewer terminal arbors in layer VI, TCAs of Cx*NR1*KO mice continue their expansion and branching in other layers (Figs. 4, 5C,D). Quantitative analyses of numbers of bifurcation points and terminal tips of TCAs in different cortical layers in Cx*NR1*KO and control mice revealed significant differences (Fig. 6). In control animals, bifurcation points and terminal tips were mostly distributed in layer IV (about 75–80% of the total number), with some in layer VI (10–15%). However, in Cx*NR1*KO cases from P5 and on, significantly ($P < 0.01$, Student's *t*-test) reduced numbers of both bifurcation points and terminal tips were counted in layer IV. On the other hand, greatly ($P < 0.05$, Student's *t*-test) increased bifurcations of TCAs, as well as their terminals, were found in layers II/III and V in Cx*NR1*KO cortices at P3 and older ages. The mediolateral extent of the TCAs in the KO cortex is significantly ($P < 0.001$, Student's *t*-test) larger than controls from P3 and on (Fig. 7). Interestingly, total numbers of bifurcation points and terminal tips in all cortical layers for each age did not show any

significant differences (Table 2). On the other hand, when we determined the total axonal branch length within the terminal field of all reconstructed single axons for each age, we found that this number was significantly higher in Cx*NR1*KO cases beginning on P5 (Table 2). This increase indicates that as the terminal arbors begin shaping, terminal branch segments get longer, thereby contributing to the wider span of terminal arbors seen in Cx*NR1*KO animals.

Despite their exuberance, Cx*NR1*KO mouse TCAs develop condensations of terminals, albeit smaller than controls, in layer IV (Fig. 8). These focal terminals, within an expansive terminal arbor, correspond to CO dense regions seen in the KO cortex, which are smaller than those seen in control mice (Fig. 8C).

DISCUSSION

In the present study, we examined detailed morphology of single TCAs in the Cx*NR1*KO somatosensory cortex during the first postnatal week. TCA arbor and terminal development of Cx*NR1*KO mice appears similar to that of control mice at P1, but by P3 significant differences begin emerging. We found that Cx*NR1*KO TCAs have longer terminal branch lengths (at P5 and P7) and wider spans laterally and radially (after P3) than WT TCAs. These differences in mediolateral extent of arbor fields and number of branch points and terminals in different cortical laminae are further accentuated between P5 and P7, when barrels normally appear as cytoarchitectonic units and become distinct (Rice et al., 1985). Previously, we showed that in Cx*NR1*KO mice *NR1* expression in the VB and all other subcortical structures are not altered, but it is abolished in the excitatory neurons of the neocortex, hippocampus, and the olfactory bulb (Iwasato et al., 2000). Exuberant terminal arbor development from VB projections to the *NR1* impaired neocortex indicates that postsynaptic NMDARs play an important role in refinement of presynaptic TCA arbors in the barrel cortex.

In an earlier study we showed that cellular modules and dendritic field orientation never develop in the Cx*NR1*KO barrel cortex (Datwani et al., 2002a). In that study, we also presented preliminary evidence from very few single axons (7 and 8 axons at P5), which suggested that Cx*NR1*KO TCAs developed smaller and rudimentary arbors. However, those few axons were reconstructed from thalamocortical slices that had not been optimized for the age-specific planes of section. Detailed analyses performed in the present study and examination of more than a dozen axons with more complete fills for each age group now indicate that Cx*NR1*KO TCAs have much wider spans laterally and radially. In addition, branch segments and total axonal length within a terminal field are longer. Our present results coupled with our previous report on the dendritic defects in layer IV spiny stellate cells of the Cx*NR1*KO cortex (Datwani et al., 2002a) show that cortical NMDAR activity plays a major role in sculpting both TCA terminal arbors and dendrites of barrel cells.

Normal development of whisker-specific TCA arbors in mice has been described (Senft and Woolsey, 1991; Agmon et al., 1995; Rebsam et al., 2002), and the present results from control cases confirm these findings. Briefly, topographically organized TCAs invade the cortical plate above layer V by P1 as simple axons with very few branches. As barreloids develop in the thalamus, their axonal terminal fields and arbors partition into “Gaussian” patches in the newly formed layer IV by P3 (Senft and Woolsey, 1991), before the barrels appear as cytoarchitectonic modules. Barrels then form around the patchy TCA terminal fields by P5. Between P3–7, there is selective pruning of overshooting collaterals, while more branches are added and consolidated within the foci of terminal patches. As noted by Senft and Woolsey earlier (1991), focal arborization is pronounced within the center of each whisker-specific Gaussian distribution of TCA terminals. Here we show by single TCA

labeling that focalization of whisker-specific TCA terminal fields still takes place, albeit to a limited extent, when subcortical NMDAR function is intact and cortical NMDAR function is impaired. These patches correspond to the rudimentary patterns seen with CO histochemistry or 5-HTT immunostaining that are commonly used as markers of barrel/TCA patterns. Cx*NR1*KO mice were generated using the Cre/loxP system. The expression of Cre recombinase gene is driven by the promoter of homeobox gene *Emx1,* which is expressed specifically in the dorsal telencephalon. GABAergic inhibitory interneurons migrate into the neocortex from the *Emx1* negative ganglionic eminence of the ventral telencephalon (Anderson et al., 1997). Therefore, in these mice GABAergic cortical neurons escape the *NR1* gene excision. GABAergic cells reportedly comprise 13–15% of barrel cells and are located along the barrel walls, with their dendrites oriented toward barrel hollows (Lin et al., 1985). Therefore, it is possible that spared NMDAR function in GABAergic barrel cortex cells might contribute to rudimentary segregation of large whisker TCA terminals within an expansive terminal arbor field.

Our findings that the total number of branch points and terminal tips do not significantly differ between Cx*NR1*KO and control mice suggest that these parameters might be intrinsically programmed in VB cells and their axons. However, we do not have any direct evidence for this scenario. Similarly, increased total branch length in Cx*NR1*KO TCA terminal arbors indicates that postsynaptic NMDAR signaling might serve a regulatory function in terminal elaboration and axon growth vigor. Postsynaptic NMDARs have been demonstrated to limit the afferent extension in vitro (Baird et al., 1996). During early development, NMDARs may function as axonal sprouting suppressors when AMPARs are not yet recruited (Lin and Constantine-Paton, 1998). At present, we do not know the precise molecular chain of events that restrict axonal/terminal branch elongation and induce localized elaboration through activation of postsynaptic NMDARs. Previously it was reported that calcium/calmodulin dependent protein kinase II (CaMKII), a key player downstream of the NMDAR-mediated signaling, might regulate the growth of tadpole retinotectal afferents. When postsynaptic CaMKII is inhibited, the growth restriction of presynaptic afferents is released, leading to the increased axonal extension (Zou and Cline, 1999).

Because in Cx*NR1*KO mice functional NMDARs are lacking in excitatory postsynaptic cells, while the parent cells of TCAs in VB have normal levels of NMDAR function, there must be retrograde signals generated downstream of NMDAR activation and consequent Ca^{2+} entry at the postsynaptic site. In fact, many lines of evidence indicate the involvement of retrograde signals in shaping afferent morphology in the vertebrate central nervous system (see reviews: Fitzsimonds and Poo, 1998; Debski and Cline, 2002). Currently, there are numerous candidate retrograde signals and synaptic molecules that could participate in this highly complex, activity-driven communication between pre- and postsynaptic elements that eventually influence their morphological and consequently functional differentiation. Nitric oxide (NO), brain-derived neurotrophic factor (BDNF), and arachidonic acid (AA) have all been implicated as potential retrograde signals that could modulate stabilization and consolidation of synapses, thereby sculpting presynaptic terminal and postsynaptic dendritic patterns (see Schmidt, 2004, for a review).

Spatial and temporal distribution of NMDARs has drawn attention in recent years (see reviews: Carroll and Zukin, 2002; Wenthold et al., 2003). As transmembrane proteins, NMDARs anchor other cell surface proteins to many other cytoplasmic molecules (reviewed by Scheiffele, 2003). Pharmacological blockade studies mainly examining the channel properties of NMDARs might not cover this aspect of NMDAR function. NR2 subunit of NMDAR binds to PDZ domains of PSD-95 (Kornau et al., 1995), the major scaffolding protein for assembly of signaling complex and cell surface molecules (Garner et al., 2000),

such as neuroligins. Neuroligins interact with neurexins to form calcium-dependent heterophilic adhesion molecules (Nguyen and Südhof, 1997), and induce presynaptic differentiation (Scheiffele et al., 2000). In addition, EphB2 can interact directly with NR1 subunit and regulate the formation of excitatory synapses through the Ephrin-EphB signaling pathway (Dalva et al., 2000).

To date, several mutant mice have been described with specific deficits in TCA terminal patterning, cellular patterning, or both, in the somatosensory cortex. In some of these mice, TCAs form partial or full whisker-specific patterns, but layer IV stellate cells do not. In others, both TCAs and stellate cells fail to develop patterns (reviewed in Erzurumlu and Kind, 2001; López-Bendito and Molnár, 2003). These mutations involve various aspects of glutamatergic synaptic communication and its regulation by 5-HT (Cases et al., 1996; Iwasato et al., 1997, 2000; Vitalis et al., 1998; Hannan et al., 1998, 2001; Salichon et al., 2001; Datwani et al., 2002a). In vitro recordings from thalamocortical slices indicated that 5-HT has a strong presynaptic inhibitory effect on glutamatergic transmission between somatosensory thalamic axons and barrel cortex cells via the activation of 5-HT1B receptors (Rhoades et al., 1994). Collectively, these data indicate that thalamocortical axons autoregulate their glutamatergic transmission via presynaptic mechanisms using 5-HT present in their target field (Persico et al., 2001). Deletions of several intracellular signaling molecules downstream from glutamate and 5-HT also show defects in barrel formation (reviewed in Erzurumlu and Kind, 2001; Gaspar et al., 2003). Rebsam et al. (2002) described the TCA arbors in monoamine oxidase A (MAOA) KO and MAOA/5-HT1B receptor double KO mice. They found that in MAOA KO and MAOA/5-HT1B double KO mice, TCAs reach the proper region and laminae of the somatosensory cortex by P1 as in normal mice. At P7, however, while whisker-specific TCA terminals are restricted to a single barrel in control animals, there was a significant reduction of terminal branches (by half) in layer IV and a 40% increase in the mediolateral span of TCA arbors in MAOA KO mice. In double KO animals, on the other hand, these defects were corrected and their TCAs attained “normal” span and terminal distribution by P7. Our present results corroborate their observations in normal/control mice, and further show that when excitatory cortical cells lack functional NMDARs, TCAs also develop expansive arbors and form terminals in multiple cortical layers instead of clustering their terminals into patches in layer IV. Intracellular signaling pathways downstream from NMDARs (or metabotropic glutamate receptors and serotonergic modulation of glutamatergic transmission), which lead to specific communication between pre- and postsynaptic elements in the barrel cortex during whisker-specific pattern formation, are largely unknown, while adenylyl cyclase type I, phospholipase $C_{\beta 1}$, cAMP response element-binding protein (CREB), and BDNF have been implicated (reviewed in Erzurumlu and Kind, 2001; Gaspar et al., 2003).

In recent years, some groups have attempted to identify cortical lamina-specific molecular signals that direct TCAs to layer IV (and to a lesser degree to layer VI), and induce them to stop there, branch, and arborize (see Yamamoto, 2002, for a review). While several in vitro models have indicated the presence of targeting and “stop” signals in layer IV (Molnár and Blakemore, 1991; Emerling and Lander, 1994; Yamamoto et al., 1997), the molecular identity of this signal and its in vivo function remains to be solved. Our present results indicate that in the absence of postsynaptic NMDAR function in excitatory cortical cells, TCA terminals explore other cortical layers, branch, and terminate therein, “ignoring” lamina specific “stop” signals. Not only in Cx*NR1*KO mice, but also in other mouse mutants with TCA terminal arbor expansions, such as the barrelless (brl or adenylyl cyclase Type 1KO) and MAOAKO, TCA terminals expand beyond layer IV (Welker et al., 1996; Rebsam et al., 2002). On the other hand, in all these mutants, and in cortical molecular mapping studies, it is evident that TCAs from different thalamic nuclei respect cortical areal

boundaries defined by molecular markers (Rubenstein et al., 1999; Grove and Fukuchi-Shimogori, 2003; Vanderhaeghen and Polleux, 2004).

In Cx*NR1*KO mice, the absence of NMDAR function in spiny stellate cells of layer IV and other excitatory neurons in the barrel field most likely impairs several downstream signals that enable postsynaptic cells to detect incoming correlated activity from TCAs and lead to aberrant dendritic differentiation as well as exuberant spine formation that could not be stabilized (Datwani et al., 2000a). Lack of NMDAR-dependent retrograde signals that regulate growth potential and focalization of TCA terminal branches would lead to expansion of TCA terminals into other layers and laterally wider areas in search of such signals. If this scenario were correct, then one would expect a high turnover of synaptic contacts (transient synapses), and a dynamic attempt at the postsynaptic site to offer more dendritic spines with relatively little success in synapse consolidation. Further studies at the ultrastructural and physiological levels would resolve this issue.

Acknowledgments

We thank Ms. Barri King for help with breeding and genotyping mice, Baris Yig it for help with axon reconstructions, and Ryan Couvillion for histology.

Grant sponsor: National Institutes of Health; Grant number: NS 039050 (to R.S.E.); Grant sponsor: Ministry of Education, Science, Sports and Culture of Japan (Grant-in-Aid for Scientific Research to T.I.).

LITERATURE CITED

Agmon A, Connors BW. Thalamocortical responses of mouse somatosensory (barrel) cortex in vitro. Neuroscience. 1991; 41:365–379. [PubMed: 1870696]

Agmon A, Yang LT, Jones EG, O'Dowd DK. Topological precision in the thalamic projection to neonatal mouse barrel cortex. J Neurosci. 1995; 15:549–561. [PubMed: 7823163]

Anderson SA, Eisenstat DD, Shi L, Rubensterin JLR. Interneuron migration from basal forebrain to neocortex: dependence on Dlx genes. Science. 1997; 278:474–476. [PubMed: 9334308]

Baird DH, Trehkner E, Mason CA. Arrest of afferent axon extension by target neurons in vitro is regulated by the NMDA receptor. J Neurosci. 1996; 16:2642–2648. [PubMed: 8786440]

Carroll RC, Zukin RS. NMDA-receptor trafficking and targeting: implications for synaptic transmission and plasticity. Trends Neurosci. 2002; 25:571–577. [PubMed: 12392932]

Cases O, Vitalis T, Seif I, De Maeyer E, Sotelo C, Gaspar P. Lack of barrels in the somatosensory cortex of monoamine oxidase A-deficient mice: role of a serotonin excess during the critical period. Neuron. 1996; 16:297–307. [PubMed: 8789945]

Dalva MB, Takasu MA, Lin MZ, Shamah SM, Hu L, Gale NW, Greenberg ME. EphB receptors interact with NMDA receptors and regulate excitatory synapse formation. Cell. 2000; 103:945–956. [PubMed: 11136979]

Datwani A, Iwasato T, Itohara S, Erzurumlu RS. NMDA receptor-dependent pattern transfer from afferents to postsynaptic cells and dendritic differentiation in the barrel cortex. Mol Cell Neurosci. 2002a; 21:477–492. [PubMed: 12498788]

Datwani A, Iwasato T, Itohara S, Erzurumlu RS. Lesion-induced thalamocortical axonal plasticity in the S1 cortex is independent of NMDA receptor function in excitatory cortical neurons. J Neurosci. 2002b; 22:9171–9175. [PubMed: 12417641]

Debski EA, Cline HT. Activity-dependent mapping in the retinotectal projection. Curr Opin Neurobiol. 2002; 12:93–99. [PubMed: 11861170]

Emerling DE, Lander AD. Laminar specific attachment and neurite outgrowth of thalamic neurons on cultured slices of developing cerebral cortex. Development. 1994; 125:3399–3410.

Erzurumlu RS, Jhaveri S. Thalamic axons confer a blueprint of the sensory periphery onto the developing rat somatosensory cortex. Dev Brain Res. 1990; 56:229–234. [PubMed: 2261684]

Erzurumlu RS, Jhaveri S. Trigeminal ganglion cell processes are spatially ordered prior to the differentiation of the vibrissa pad. J Neurosci. 1992a; 12:3946–3955. [PubMed: 1403092]

Erzurumlu RS, Jhaveri S. Emergence of connectivity in the embryonic rat parietal cortex. Cereb Cortex. 1992b; 2:336–352. [PubMed: 1422091]

Erzurumlu RS, Kind PC. Neural activity: sculptor of “barrels” in the neocortex. Trends Neurosci. 2001; 24:589–595. [PubMed: 11576673]

Erzurumlu RS, Jhaveri S, Benowitz LI. Transient patterns of GAP-43 expression during the formation of barrels in the rat somatosensory cortex. J Comp Neurol. 1990; 292:443–456. [PubMed: 2160480]

Fitzsimonds RM, Poo MM. Retrograde signaling in the development and modification of synapses. Physiol Rev. 1998; 78:143–170. [PubMed: 9457171]

Garner CC, Nash J, Huganir RL. PDZ domains in synapse assembly and signaling. Trends Cell Biol. 2000; 10:274–280. [PubMed: 10856930]

Gaspar P, Cases O, Maroteaux L. The developmental role of serotonin: news from mouse molecular genetics. Nat Rev Neurosci. 2003; 4:1002–1012. [PubMed: 14618156]

Grove EA, Fukuchi-Shimogori T. Generating the cerebral cortical area map. Annu Rev Neurosci. 2003; 26:355–380. [PubMed: 14527269]

Hannan AJ, Kind PC, Blakemore C. Phospholipase C-beta1 expression correlates with neuronal differentiation and synaptic plasticity in rat somatosensory cortex. Neuropharmacology. 1998; 7:593–605. [PubMed: 9705000]

Hannan AJ, Blakemore C, Katsnelson A, Vitalis T, Huber KM, Near M, Roder J, Kim D, Shin HS, Kind PC. PLC-β1, activated via mGluRs, mediates activity-dependent differentiation in cerebral cortex. Nat Neurosci. 2001; 4:282–288. [PubMed: 11224545]

Iwasato T, Erzurumlu RS, Huerta PT, Chen DF, Sasaoka T, Ulupinar E, Tonegawa S. NMDA receptor-dependent refinement of somatotopic maps. Neuron. 1997; 19:1201–1210. [PubMed: 9427244]

Iwasato T, Datwani A, Wolf AM, Nishiyama H, Taguchi Y, Tonegawa S, Knõpfel T, Erzurumlu RS, Itohara S. Cortex-restricted disruption of NMDAR1 impairs neuronal patterns in the barrel cortex. Nature. 2000; 406:726–731. [PubMed: 10963597]

Killackey HP, Rhoades RW, Bennett-Clarke CA. The formation of a cortical somatotopic map. Trends Neurosci. 1995; 18:402–407. [PubMed: 7482806]

Kornau H-C, Schenker LT, Kennedy MB, Seeburg PH. Domain interaction between NMDA receptor subunits and postsynaptic density protein PSD-95. Science. 1995; 269:1737–1740. [PubMed: 7569905]

Kutsuwada T, Sakimura K, Manabe T, Takayama C, Katakura N, Kushiya E, Natsume R, Watanabe M, Inoue Y, Yagi T, Aizawa S, Arakawa M, Takahashi T, Nakamura Y, Mori H, Mishina M. Impairment of suckling response, trigeminal neuronal pattern formation, and hippocampal LTD in NMDA receptor epsilon 2 subunit mutant mice. Neuron. 1996; 16:333–344. [PubMed: 8789948]

Lebrand C, Cases O, Adelbrecht C, Doye A, Alvarez C, El Mestikawy S, Seif I, Gaspar P. Transient uptake and storage of serotonin in developing thalamic neurons. Neuron. 1996; 17:823–835. [PubMed: 8938116]

Lebrand C, Case O, Wehrle R, Blakely RD, Edwards RH, Gaspar P. Transient developmental expression of monoamine transporters in the rodent forebrain. J Comp Neurol. 1998; 401:506–524. [PubMed: 9826275]

Li Y, Erzurumlu RS, Chen C, Jhaveri S, Tonegawa S. Whisker-related neuronal patterns fail to develop in the trigeminal brainstem nuclei of NMDAR1 knockout mice. Cell. 1994; 76:427–437. [PubMed: 8313466]

Lin CS, Lu SM, Schmechel DE. Glutamic acid decarboxylase immunoreactivity in layer IV of barrel cortex of rat and mouse. J Neurosci. 1985; 5:1934–1939. [PubMed: 2991479]

Lin SY, Constantine-Paton M. Suppression of sprouting: an early function of NMDA receptors in the absence of AMPA/Kainate receptor activity. J Neurosci. 1998; 18:3725–3737. [PubMed: 9570803]

López-Bendito G, Molnár Z. Thalamocortical development: how are we going to get there? Nat Rev Neurosci. 2003; 4:276–289. [PubMed: 12671644]

Ma PM, Woolsey TA. Cytoarchitectonic correlates of the vibrissae in the medullary trigeminal complex of the mouse. Brain Res. 1984; 306:374–379. [PubMed: 6205721]

Maier DL, Mani S, Donovan SL, Soppet D, Tessarollo L, McCasland JS, Meiri KF. Disrupted cortical map and absence of cortical barrels in growth-associated protein (GAP)-43 knockout mice. Proc Natl Acad Sci U S A. 1999; 96:9397–9402. [PubMed: 10430954]

Molnár Z, Blakemore C. Lack of regional specificity for connections formed between thalamus and cortex in coculture. Nature. 1991; 351:475–477. [PubMed: 2046749]

Nguyen T, Südhof TC. Binding properties of neuroligin 1 and neurexin 1 beta reveal function as heterophilic cell adhesion molecules. J Biol Chem. 1997; 272:32–39. [PubMed: 8995221]

O'Leary DDM, Ruff NL, Dyck RH. Development, critical period plasticity, and adult reorganizations of mammalian somatosensory systems. Curr Opin Neurobiol. 1994; 4:535–544. [PubMed: 7812142]

Persico AM, Mengual E, Moessner R, Hall FS, Revay RS, Sora I, Arellano J, DeFelipe J, Gimenez-Amaya JM, Conciatori M, Marino R, Baldi A, Cabib S, Pascucci T, Uhl GR, Murphy DL, Lesch KP, Keller F, Hall SF. Barrel pattern formation requires serotonin uptake by thalamocortical afferents, and not vesicular monoamine release. J Neurosci. 2001; 21:6862–6873. [PubMed: 11517274]

Rebsam A, Seif I, Gaspar P. Refinement of thalamocortical arbors and emergence of barrel domains in the primary somatosensory cortex: a study of normal and monoamine oxidase a knock-out mice. J Neurosci. 2002; 22:8541–8552. [PubMed: 12351728]

Rhoades RW, Bennett-Clarke CA, Shi MY, Mooney RD. Effects of 5-HT on thalamocortical synaptic transmission in the developing rat. J Neurophysiol. 1994; 72:2438–2450. [PubMed: 7884470]

Rice FL, Gomez C, Barstow C, Burnet A, Sands P. A comparative analysis of the development of the primary somatosensory cortex: interspecies similarities during barrel and laminar development. J Comp Neurol. 1985; 236:477–495. [PubMed: 4056099]

Rubenstein JLR, Anderson S, Shi L, Miyashita-Lin E, Bulfone A, Hevner R. Genetic control and regionalization and connectivity. Cereb Cortex. 1999; 9:524–532. [PubMed: 10498270]

Salichon N, Gaspar P, Upton AL, Picaud S, Hanoun N, Hamon M, De Maeyer E, Murphy DL, Mossner R, Lesch KP, Hen R, Seif I. Excessive activation of serotonin (5-HT) 1B receptors disrupts the formation of sensory maps in monoamine oxidase A and 5-HT transporter knock-out mice. J Neurosci. 2001; 21:884–896. [PubMed: 11157075]

Scheiffele P. Cell-cell signaling during synapse formation in the CNS. Annu Rev Neurosci. 2003; 26:485–508. [PubMed: 12626697]

Scheiffele P, Fan J, Choih J, Fetter R, Serafini T. Neuroligin expressed in nonneuroal cells triggers presynaptic development in contacting axons. Cell. 2000; 101:657–669. [PubMed: 10892652]

Schmidt JT. Activity-driven sharpening of the retinotectal projection: the search for retrograde synaptic signaling pathways. J Neurobiol. 2004; 59:114–133. [PubMed: 15007831]

Senft SL, Woolsey TA. Growth of thalamic afferents into mouse barrel cortex. Cereb Cortex. 1991; 1:308–335. [PubMed: 1822738]

Van der Loos H. Barreloids in mouse somatosensory thalamus. Neurosci Lett. 1976; 2:1–6. [PubMed: 19604804]

Vanderhaeghen P, Polleux F. Developmental mechanisms patterning thalamocortical projections: intrinsic, extrinsic and in between. Trends Neurosci. 2004; 27:384–391. [PubMed: 15219737]

Vitalis T, Cases O, Callebert J, Launay JM, Price DJ, Seif I, Gaspar P. Effects of monoamine oxidase A inhibition on barrel formation in the mouse somatosensory cortex: determination of a sensitive developmental period. J Comp Neurol. 1998; 393:169–184. [PubMed: 9548695]

Welker E, Van der Loos H. Quantitative correlation between barrel-field size and the sensory innervation of the whiskerpad: a comparative study in six strains of mice bred for different patterns of mystacial vibrissae. J Neurosci. 1986; 6:3355–3373. [PubMed: 3772437]

Welker E, Armstrong-James M, Bronchti G, Ourednik W, Gheorghita-Baechler F, Dubois R, Guernsey DL, Van der Loos H, Neumann PE. Altered sensory processing in the somatosensory cortex of the mouse mutant barrelless. Science. 1996; 271:1864–1867. [PubMed: 8596955]

Wenthold RJ, Prybylowski K, Standley S, Sans N, Petralia RS. Trafficking of NMDA receptors. Annu Rev Pharmacol Toxicol. 2003; 43:335–358. [PubMed: 12540744]

Woolsey, TA. Peripheral alteration and somatosensory development. In: Coleman, EJ., editor. Development of sensory systems in mammals. New York: John Wiley & Sons; 1990. p. 461-516.

Woolsey TA, Van der Loos H. The structural organization of layer IV in the somatosensory region (SI) of mouse cerebral cortex. The description of a cortical field composed of discrete cytoarchitectonic units. Brain Res. 1970; 17:205–242. [PubMed: 4904874]

Yamamoto N. Cellular and molecular basis for the formation of lamina-specific thalamocortical projections. Neurosci Res. 2002; 42:167–173. [PubMed: 11900826]

Yamamoto N, Higashi S, Toyama K. Stop and branch behaviors of geniculocortical axons: a time-lapse study in organotypic cocultures. J Neurosci. 1997; 17:3653–3663. [PubMed: 9133388]

Zou DJ, Cline HT. Postsynaptic calcium/calmodulin-dependent protein kinase II is required to limit elaboration of presynaptic and postsynaptic neuronal arbors. J Neurosci. 1999; 19:8909–8918. [PubMed: 10516310]

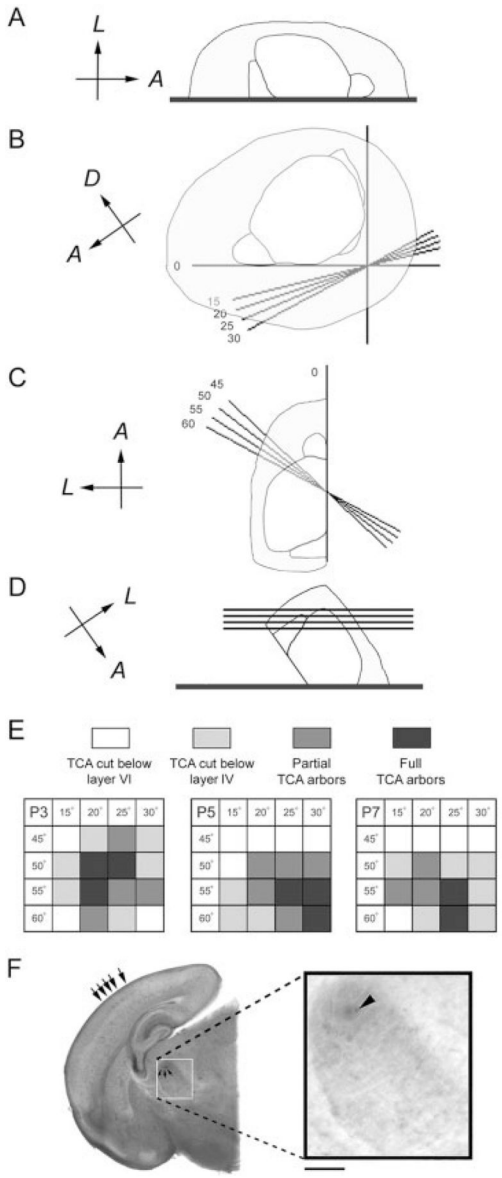

Fig. 1.

Optimal angles for preparation of intact thalamocortical pathway slices at different developmental ages. Oblique planes of sectioning parallel to the thalamocortical pathway were used for different postnatal ages. The forebrains were split in half along the sagittal plane, and each hemisphere was embedded in 2% agar with the medial side down (**A**). The specimen was placed on an X-Y coordinate, with the occipital pole contacting the Y-axis, and the plane along the olfactory bulb and the base of the forebrain aligned with the X-axis. Different cutting angles (15, 20, 25, or 30° deviating from the X-axis) were tested; the cuts were made through the agar block (**B**). The specimen was lifted with a spatula from its ventral side. Different oblique angles of cuts (45, 50, 55, or 60° deviating from the Y-axis) were tested (**C**). The rostral pole of the block was mounted down to the vibratome stage and the tissue block was cut from the caudal pole (**D**). The gray scale codes are used to illustrate the results. When a single TCA could be traced from the internal capsule to a CO-dense single patch in layer IV, the plane was designated as optimal (the darkest color) (**E**). A

typical example of a thalamocortical slice with DiI implant in the barreloid region of the VB is illustrated for a P5 case (**F**). Arrows point to barrels in the cortex and barreloids in the VB. Inset shows higher magnification view of the DiI implant (arrowhead). Scale bars = 200 μm in the inset; 1 mm in A–D.

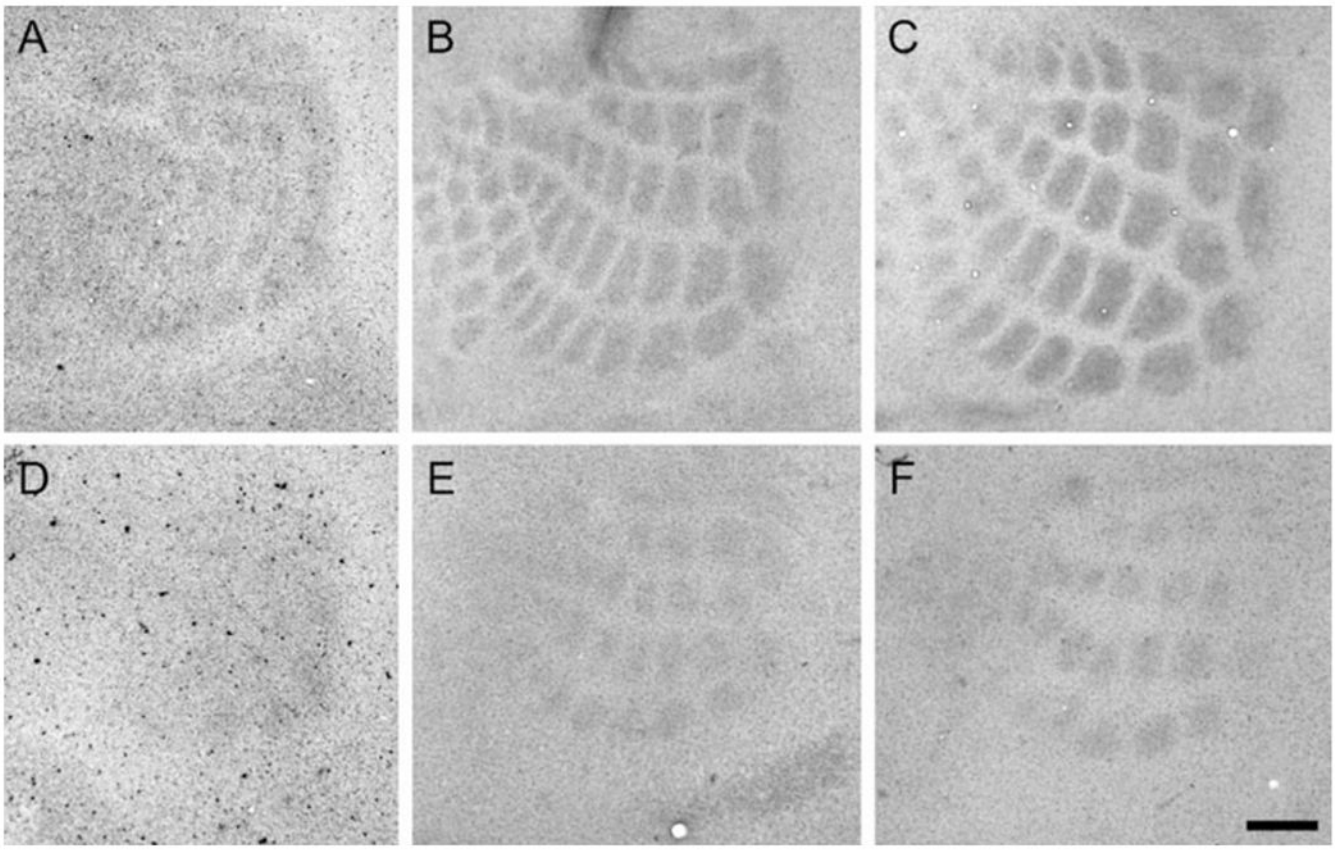

Fig. 2.

Development of TCA patches in normal and Cx*NR1*KO barrel cortex as revealed with 5-HTT immunohistochemistry. Tangential sections of flattened cortices at ages P3 (**A** and **D**), P5 (**B** and **E**), and P7 (**C** and **F**) are collected from control (A–C) and Cx*NR1*KO (D–F) mice. Whisker-specific patterns of 5-HTT-positive TCAs appear in the normal somatosensory cortex as early as P3 (A), and become more distinctive as the brain develops (B, C). However, the patterns are less discernible in the Cx*NR1*KO cortex at P3 (D). At later ages, smaller TCA patches become visible in the major whisker representation area (E, F). Scale bar = 100 μm in F (applies to A–F).

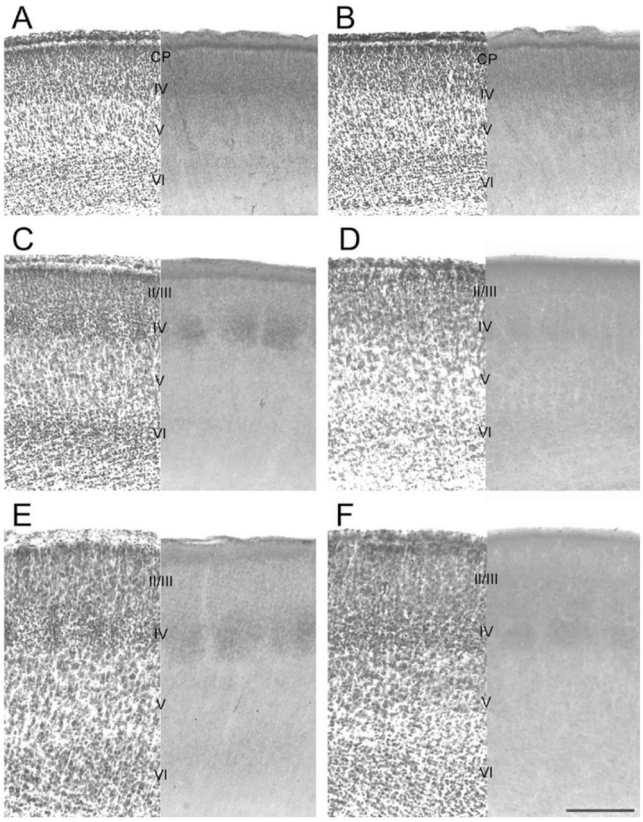

Fig. 3.

Delineation of cortical laminae at various developmental ages with adjacent sections stained for Nissl (left) and CO (right). Sections were cut according to the optimal angles at P3 (**A** and **B**), P5 (**C** and **D**), and P7 (**E** and **F**) and stained with Nissl and CO. Cortical layers are revealed by both staining methods in control (A, C, E) and Cx*NR1*KO (B, D, F) mouse brains. Note the cell-dense barrel walls in Nissl-stained control cortices (C, E) and their absence in Cx*NR1*KO brains, and normal CO patches in control cortex and smaller CO patches in Cx*NR1*KO mice. Scale bar = 200 μm in F (applies to A–F).

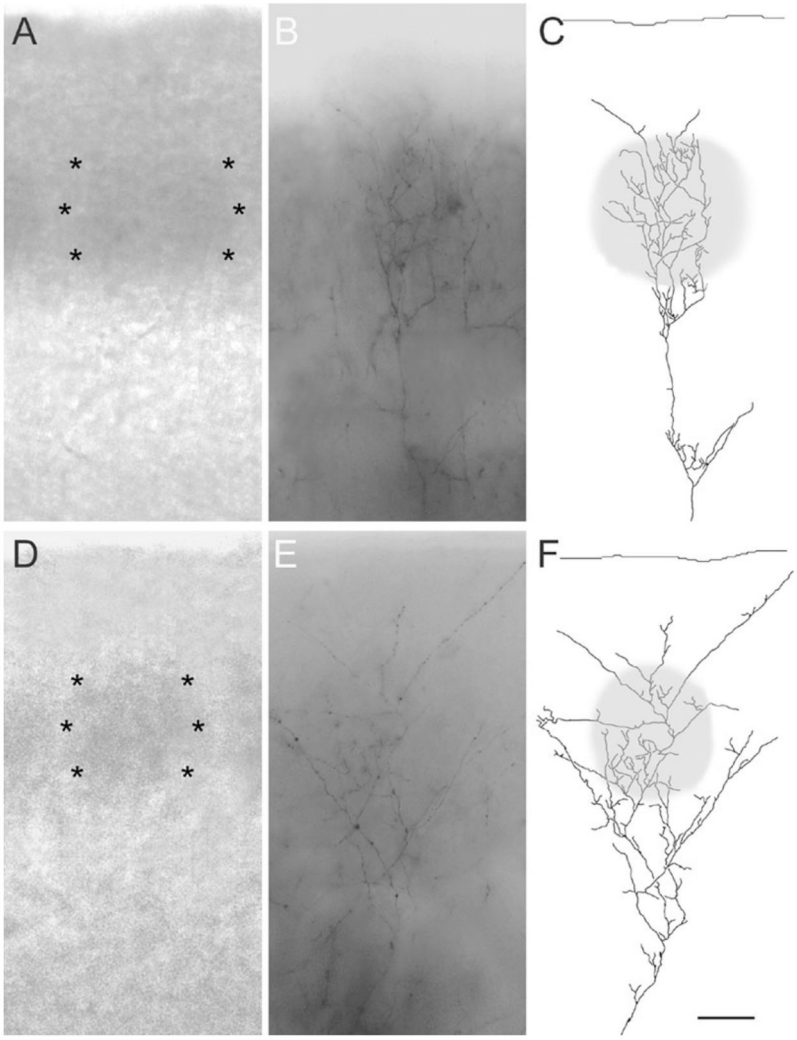

Fig. 4.

DiI-labeled single axons in CO-stained thalamocortical slices. A small crystal of DiI was inserted into the barreloid region of a slightly CO stained thalamocortical section; single TCAs were then visualized and traced. Examples of control (**A–C**) and Cx*NR1*KO (**D–F**) P7 TCA are presented. Cortical layers and barrel patterns are revealed by CO staining (A, D, asterisks). Single TCAs in the somatosensory cortex are labeled with DiI. Images from different focal planes were collected and superimposed, then converted into black-and-white for better resolution (B, E). Tracings of single TCAs were made manually based on the reconstructed images (C, F). Single patches (gray in C, F) from CO-stained sections (A, D) were pasted on the afferent arbor indicating the relative position of the CO-dense patches with respect to TCA terminal arbor fields. Scale bar = 100 μm in F (applies to A–F).

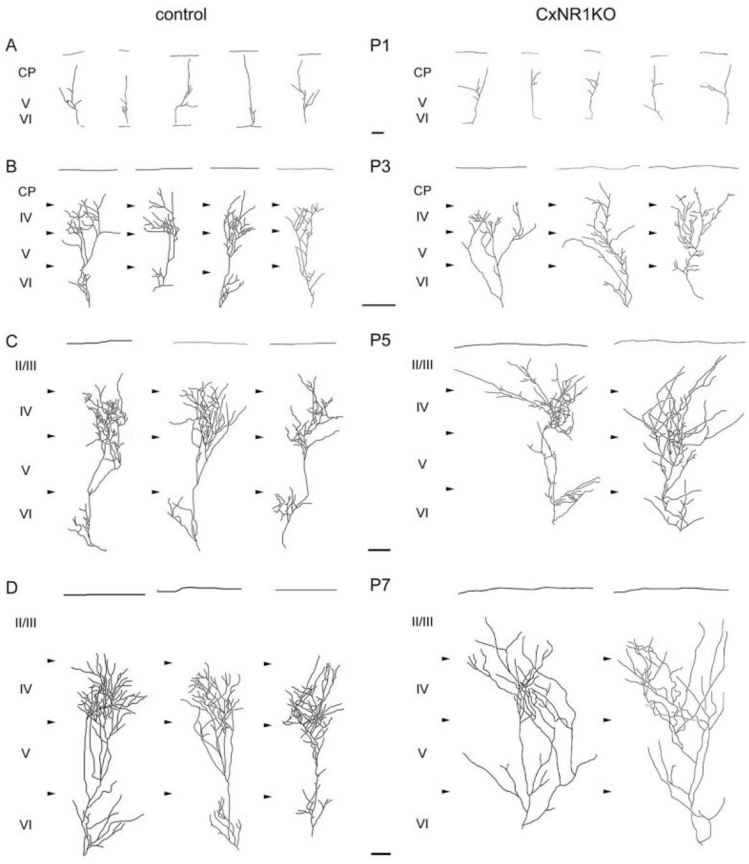

Fig. 5.

Examples of single TCA arbors in control and Cx*NR1*KO cortex between P1–7. At P1, TCAs invade the cortical plate (CP) as simple axons with few small branches in both control and Cx*NR1*KO cases (**A**). On P3, TCAs display focalized branches in layer IV and a few in layer VI in control mice. Relatively few branches are seen in other layers. In Cx*NR1*KO cortex, TCAs display a wider terminal territory and more branches are present in other layers (**B**). Normal TCAs in P5 and P7 show their focal terminal arbors in layer IV and some terminal arbors in layer VI but have very few branches in other layers. TCAs of Cx*NR1*KO mice continue their lateral expansion and branching in other layers (**C** and **D**). Scale bar = 100 μm.

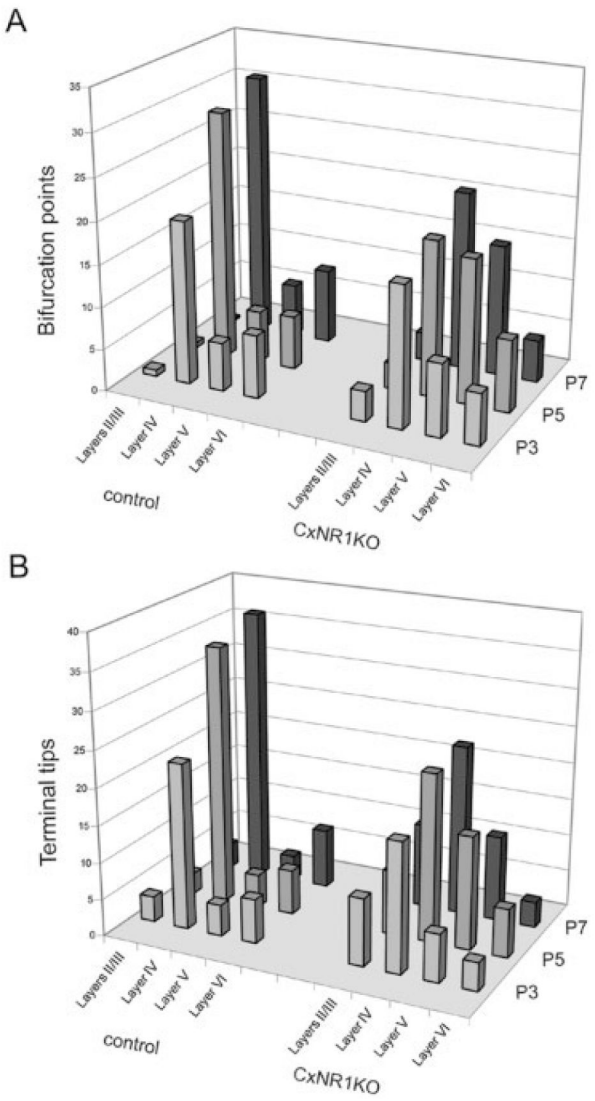

Fig. 6.

Bifurcation points and terminal tips of TCAs in different cortical layers at different postnatal ages. Numbers of bifurcation points (**A**) and terminal tips (**B**) of each reconstructed single TCA were counted in different cortical layers in Cx*NR1*KO and control mice. For bifurcation points (A), from P3 and on, TCAs of Cx*NR1*KO mice have a greater number in layers II/III and layer V than control TCAs. On the other hand, in layer IV, Cx*NR1*KO mice have fewer bifurcation points than control mice on P5 and P7. For terminal tips (B) from P3 and on, Cx*NR1*KO TCAs have a greater number in layers II/III and layer V but a lower number in layer IV than control TCAs.

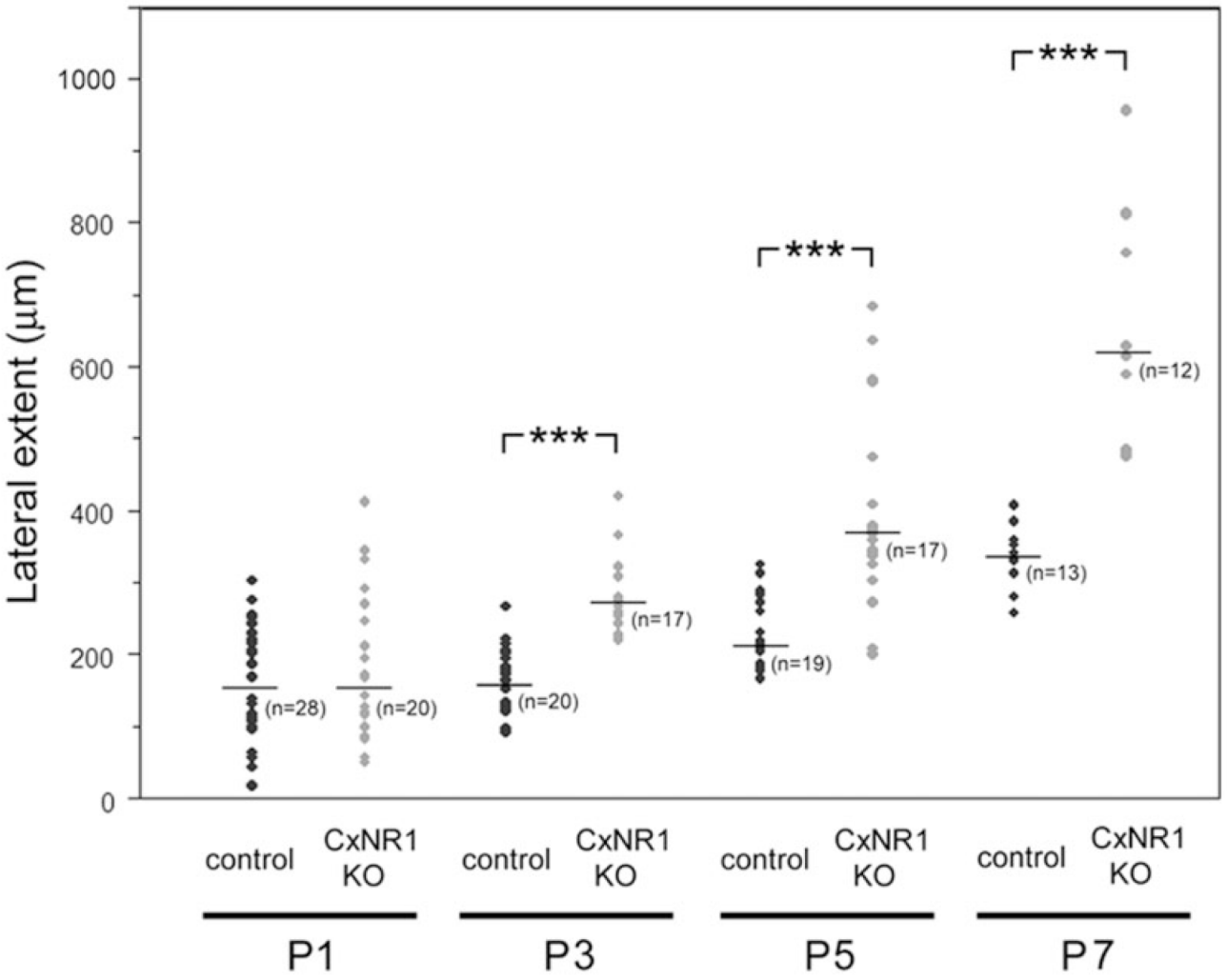

Fig. 7.

Mediolateral extent of single TCA arbors between P1–7. Lateral extent of TCAs from control (black) and Cx*NR1*KO (gray) animals were measured and plotted in groups. At P1, there is no difference between control and Cx*NR1*KO cases. However from P3 and on the mediolateral extent of the TCAs in the mutant cortex is significantly greater than those in controls. Mean value of each group is demonstrated by a horizontal bar. Significant differences are indicated by asterisks (***$P < 0.001$, Student's *t*-test).

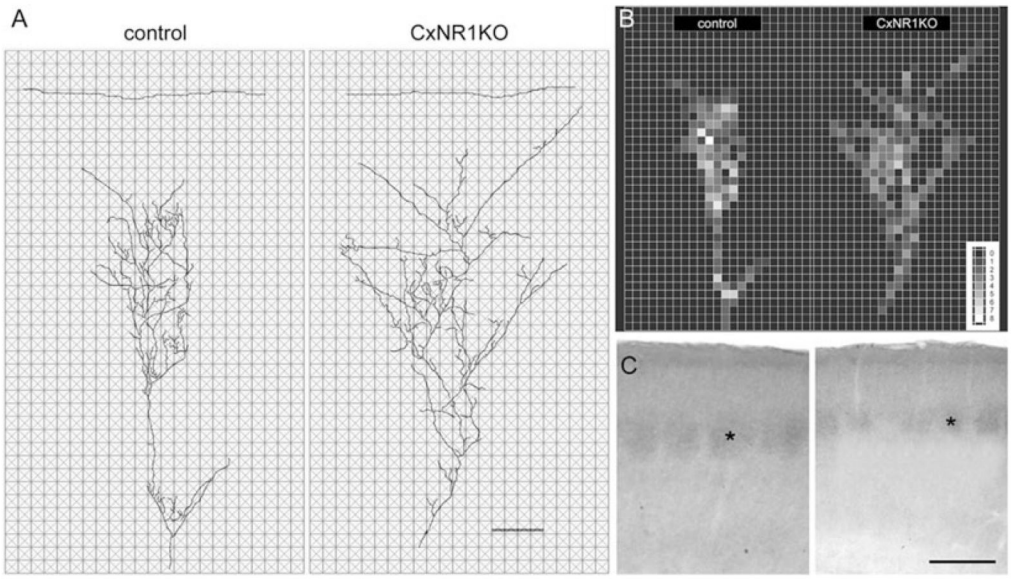

Fig. 8.

Arbor density of control and Cx*NR1*KO TCAs. The 2D density of arbors was determined by counting intersections across the two diagonals of every 25 × 25 μm^2 (**A**) and plotted in gray scale (**B**). The control case has more high-density spots (intersections greater than 5) than the Cx*NR1*KO case (16 and 2, respectively) and the profile matches the CO-stained pattern of the adjacent section (**C**, asterisk, left). Note there is some relatively higher density spots present in the Cx*NR1*KO case forming a small region matching the smaller CO-stained patches (C, asterisk, right). Scale bars = 100 μm in A; 200 μm in C.

TABLE 1

Numbers of Animals Used and TCAs Traced

	For optimal angle study			For TCAs development study			
	C57 BL/6 (wildtype)	*EmxI*$^{Cre/+}$ *NRI*$^{flox/+}$ (control)	*EmxI*$^{Cre/+}$ *NRI*$^{flox/+}$ (Cx*NRI* KO)	*EmxI*$^{Cre/+}$ *NRI*$^{flox/+}$ (control)		*EmxI*$^{Cre/+}$ *NRI*$^{flox/+}$ (Cx*NRI* KO)	
	Mice used			Mice used	TCAs traced	Mice used	TCAs traced
P1	12	5	4	11	28	12	20
P3	24	8	4	38	20	30	17
P5	23	7	5	55	19	22	17
P7	24	6	6	24	13	34	12
Total	83	26	19	128	80	98	66

TABLE 2

Numbers of Terminal Endpoints, Branch Points, and Total Arbor Segment Length Between P1 and P7[1]

	Total branch points		Total terminal points		Total arbor segment length (μm)	
Age	**control**	**Cx*NRI* KO**	**control**	**Cx*NRI* KO**	**control**	**Cx*NRI* KO**
P1	2.45 ± 2.48	2.75 ± 2.53	3.58 ± 2.56	3.64 ± 2.28	652 ± 211	602 ± 228
P3	33.4 ± 10.6	34.94 ± 10.26	34.75 ± 10.93	36.88 ± 10.26	2241 ± 578.8	2489 ± 427.4
P5	42.53 ± 10.01	47.76 ± 11.4	44.31 ± 10.29	49.29 ± 11.93	3707 ± 976.3	5389 ± 1621.8**
P7	42.83 ± 11.5	40.91 ± 9.32	44.18 ± 11.02	42.17 ± 9.24	6333 ± 1750	8195 ± 1542.1*

[1]Results are mean ± SD:

*, $P < 0.05$;

**, $P < 0.01$, Student's *t*-test).